Academic Sciences

International Journal of Current Pharmaceutical Research

ISSN- 0975-7066 Vol 4, Issue 1, 2012

Research Article

MODIFYING EFFECT OF QUERCETIN ON MODEL BIOMEMBRANES: STUDIED BY MOLECULAR DYNAMIC SIMULATION, DSC AND NMR

[a]RAGINI SINHA [b]MANOJ K.GADHWAL, [b]URMILA J.JOSHI, [a*]SUDHA SRIVASTAVA AND [a@]GIRJESH GOVIL

[@]INSA Golden Jubilee Professor, [a]National Facility for High Field NMR, Tata Institute of Fundamental Research, [b]Prin K M Kundanani College of Pharmacy, Cuffe Parade, Mumbai 400005, India. Email: sudha@tifr.res.in

Received: 28 November 2011, Revised and Accepted: 22 December 2011

ABSTRACT

Quercetin (3,5,7,3′,4′-pentahydroxy flavones) is a naturally occurring flavonoid that exerts multiple pharmacological effects. However,there are challenges associated with the bioavailability of quercetin. The substituents on the flavonoid molecules largely influence the physicochemical properties and determines the partitioning into membranes. In view of this, we have modified the quercetin molecule giving rise to two analogues Q1 (4′-chloro-3-hydroxy-flavone) and Q2 (4′-methoxy-3-hydroxy-flavone). Three of the phenolic-OH groups of quercetin are eliminated and one of the phenolic-OH is substituted by -Cl and -OCH3 group to prepare Q1 and Q2, respectively. Their interaction with model membrane has been compared using MD simulations, DSC and NMR techniques. The MD simuations indicate that the phenolic-OH groups in quercetin and the methoxy group in Q2 are the major participants in the formation of H-bonds with the polar head of the lipid bilayer.Due to high energy barrier, the entry of quercetin into the lipid core is restricted. The removal of phenolic-OH groups and substitution of -OCH3 in Q2, reduces the energy barrier and leads to better penetration into the hydrophobic core. Q1 with -Cl group substitution shows lesser tendency of binding to the polar head group of lipid and remains largely in the hydrophobic core. Intermolecular NOEs from NMR spectra support these observations. Anticancer activity shown by these compounds is significant. Results indicate that the phenolic-OH groups and the type of substituent in the quercetin play an important role in its activity, interaction with membrane and may be responsible for its permeability and bioavailability.

Keywords: Quercetin, Molecular dynamic simulations, DPPC, NMR, DSC.

INTRODUCTION

Flavonoids are a group of naturally occurring, low molecular weight benzo–γ–pyrone derivatives, ubiquitous in plants. They possess several biological properties [1, 2]. These include antioxidant, anti-inflammatory and antiproliferative effects. Quercetin (3, 5, 7, 3′, 4′–pentahydroxy flavones) (Fig.1) is the most extensively explored flavonoid belonging to flavonol class. Multiple mechanisms have been identified to explain the anticancer activity of quercetin. The suppression of carcinogenesis is proposed to be due to its radical scavenging activity [3]. In addition, quercetin is reported to inhibit CYP450 family of enzymes [4], which play a major role in the activation of a number of suspected human carcinogens. Quercetin has also been shown to cause cell cycle arrest and apoptosis by a p53 dependent mechanism [5]. Inhibition of protein tyrosine kinase [6] has also been proposed as a mechanism of action. These mechanisms may be related, at least partially to their capacity to penetrate into the cell membrane and effect membrane dependent processes.

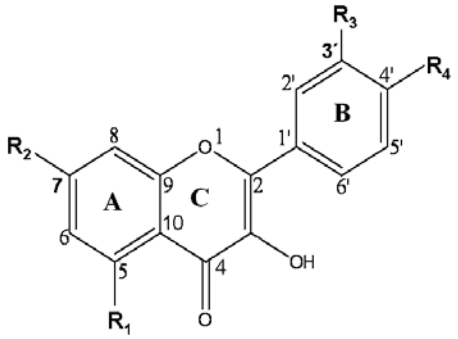

	R_1	R_2	R_3	R_4
Quercetin	OH	OH	OH	OH
Q1	H	H	H	Cl
Q2	H	H	H	OCH_3

Fig. 1: Molecular structure of quercetin and its analogues, Q1 and Q2

Biological membranes play an important role in drug transport, distribution, action, selectivity and toxicity [7, 8]. Therefore it is important to understand the molecular mechanism of interaction of flavonoids with model membrane [9]. Composition of model membranes can be controlled and they can be made to mimic biomembranes [10]. The phase transition temperature (T_m) of the model membrane plays an important role in binding, and varies depending upon the lipid composition. The model membrane prepared from dipalmitoyl phosphatidylcholine (DPPC) is ideally suited for drug–membrane interaction because of its T_m value of 314 K [11, 12] which is well above room temperature.

Quercetin consists of two aromatic rings A and B linked by an oxygen–containing heterocycle ring C. In natural form, quercetin is present as polyphenolic glycoside [13]. The glycoside is too polar to penetrate the intestinal membranes and is not easily absorbed. The release of the aglycone by the action of the microfloral enzymes is required for the compound to become absorbable. Although the aglycones are permeable, the bioavailability is low due to poor water solubility and a greater extent of conjugation which is related to multiple hydroxyl groups present in the structure. The hydroxylation degree of flavonoids is a determinant for their tendency to degradation in the colon and their degradation products produced by colonic microflora. The absence of the hydroxyl group in the molecule prevents the degradation of ring structure. The degree of hydroxylation, such as 5,7-dihydroxylation and/or 4'-hydroxylation, enhances degradation. [14]

Various synthetic 4'-substituted flavones without a single hydroxyl group are reported in the literature [15, 16]. Some of these compounds have shown promising antiproliferative activity. However there are very few reports about the structural modifications of Quercetin in order to improve its activity and bioavailability. In view of these facts we decided to modify Quercetin and synthesize 4'-substituted flavonols and study the effect of these compounds on their antiproliferative activity and membrane interactions. In preparing the two analogues Q1 and Q2, three of the phenolic–OH groups of ring A and ring B of quercetin are eliminated and one of the phenolic–OH group in ring B is replaced by a –Cl and a $–OCH_3$ group, respectively. Both the groups are likely to enhance the lipophilicity of the molecule. The 3-OH group of ring C remains unchanged.

We have attempted to correlate the behavior of the quercetin and its analogues towards DPPC considering the general hypothesis that the type of substituents on the flavonoid molecules play a crucial role in their interaction with membranes [17] and thereby affect the bioavailability of the drug. The mode of interaction of quercetin and its analogues with DPPC bilayers at molecular level has been compared using molecular dynamic simulations (MD), DSC and multinuclear NMR techniques.

MATERIALS AND METHODS

Quercetin and 1, 2–dipalmitoyl–sn–glycerol–3–phosphocholine (DPPC) were purchased from Sigma chemicals Co. USA. All the chemicals used for synthesis are from S. D. Fine chemical, India. The reagents used are of A.R. grade.

NMR experiments

NMR experiments were recorded on a BRUKER AVANCE 500 MHz NMR spectrometer. The 2D–NOESY (Nuclear Overhauser effect spectroscopy) and the ROESY (Rotating frame Overhauser effect spectroscopy) spectra were recorded using standard pulse programs [18, 19]. NOESY experiments were recorded at 323K, with a mixing time of 400ms. ^{31}P and ^{13}C NMR experiments were carried out using a relaxation delay of 1s using broadband proton decoupling. The data was processed using Topspin 2.0.

DSC experiments

DSC measurements were performed using the differential scanning calorimeter VP–DSC (Microcal, Northampton, MA, USA). The samples were degassed before being loaded into the reference and sample cells. A scan rate of 1.5ºC/ min over the temperature range 20–60ºC was employed. Repeated scans for the same samples were generally super imposable. Data were analyzed with the software ORIGIN provided by Microcal.

Sample preparation for NMR and DSC experiments

Multilamellar vesicles (MLVs) were prepared using standard procedure [20]. Samples for NMR were prepared by first dissolving the desired quantity of DPPC in chloroform along with the drug in methanol. The solvent was evaporated with a stream of nitrogen so as to deposit a lipid film on the walls of the container. Last traces of solvent were removed by vacuum drying for at least 1h. The film was hydrated with the required amount of D_2O at pH 7.2, followed by incubation in water bath at 50ºC with repeated vortexing. The lipid concentration for NMR samples was maintained at 100 mM while the drug/analog concentration was varied from 10 to 50 mM. For DSC experiments, samples were prepared by mixing the lipid and drug solutions in such a way so as to obtain mol fractions (X_D)of drugs from 0.05 to 0.5 (drug:lipid ratio from 1:20 to 1:2) by maintaining the lipid concentration to 50 mM. Unilamellar vesicles (ULVs) for NMR experiments were prepared by sonicating the above dispersions with a Branson Sonicator–450 at 50% duty cycles till optical clarity was obtained.

Determination of drug–MLV binding

Drug/analogue–MLV binding constants were determined by the centrifugation method [21]. A fixed drug concentration of 100 µM giving drug:lipid ratio of 1:2.5 to 1:20, was added systematically to varied concentration of lipid MLVs (prepared as above) in the range of 0.25mg/ml to 2mg/ml. After incubation for 2h, it was centrifuged for 0.5h at 30,000 rpm. The supernatant was taken and its optical density was measured.

The amount of compound bound to liposomes was determined from the difference in the optical density measured for the pure drug/analogue and the optical density of the supernatant. The drug–liposome apparent binding constant (k) was analyzed using a double reciprocal plot of 1/ (fraction bound) versus 1/ (lipid concentration). This yields a straight line with a slope 1/k.

TEM experiments

Experiments were performed on a Carl Zeiss Libra 120 EF TEM (Germany) with a LaB_6 emitter and 120kV accelerating voltage. Lipid samples were deposited on Formvar/carbon coated copper grids (300C–FC, Electron Microscopy Sciences, Hatfield, PA) and allowed to equilibrate. Excess liquid was removed with a filter paper and the grid was air–dried.

Computational studies

Computational studies were carried out using Desmond 2.2 running on CentOS 5.4 Linux workstation. The force field employed for the molecular dynamic simulation was OPLS. The typical system consisted of 24 DPPC molecules and 723 water molecules. Simulations were carried out in NPT (normal pressure and temperature) ensemble with the pressure coupling constant of 1.0 ps and the temperature coupling constant of 0.1 ps. The temperature and the pressure parameters were set to 323K and 1.01325 bar respectively, which are common conditions for the study of DPPC bilayers [22]. The system was coupled to a Berendsen thermostat and barostat. Periodic boundary conditions were enforced. The non–bonded cut–off was set to 9Å. All the bond lengths involving hydrogens were constrained with SHAKE algorithm. The simulated system was constructed by inserting the molecule under consideration (quercetin/Q1/Q2) into the middle of the bilayer where there is a relatively large free volume available and therefore the insert position results in least perturbation.

Similarly constructed system has been previously used to study the behavior of photosensitive molecules inside lipid bilayer [23-26]. Using this method, MD simulations have been performed to study the properties and the permeability of hypericin, substituted with bromine atoms, in a DPPC lipid membrane. The molecules were found to accumulate in the most dense region of the lipids due to competing interactions with the hydrophobic lipid interior and the polar aqueous environment [26].

In our simulation, the net charge on the system was adjusted to zero. To start the simulation, ystem was energy minimized with gradually decreasing harmonic restraints followed by a 0.5 ns relaxation to remove bad contacts by initial relaxation of the lipid and the solvent molecules, followed by relaxation of the drug/analog–lipid complex. The energy of intermolecular interaction was monitored and was found to equilibrate in this time. This was followed by a 20 ns MD simulation. The trajectories were recorded at 4.8 ps intervals.

Anticancer activity

Anticancer activity was determined by sulphorhodamine B (SRB) assay [27, 28]. The cell line (MCF-7) was grown in RPMI 1640 medium containing 10% fetal bovine serum and 2 mM L-glutamine. Cells were inoculated into 96 well microtiter plates and were incubated at 37 °C, 5 % CO_2, 95 % air and 100 % relative humidity for 24 h. Drugs were solubilized in dimethyl sulfoxide and diluted to 1 mg/ml using water. Further dilution with complete medium gave the desired concentrations of 10 µg/ml, 20 µg/ml, 40 µg/ml, 80 µg/ml. Plates were incubated for 48 hours and assay was terminated by the addition of cold TCA. SRB solution was added to each of the wells, and plates were incubated for 20 minutes at room temperature. After staining, the residual dye was removed by washing with 1 % acetic acid and air dried. Bound stain was subsequently eluted with 10 mM trizma base, and the absorbance was read at 540 nm. Percent Growth was expressed as the ratio of average absorbance of the test well to the average absorbance of the control wells *100.

Synthesis of quercetin analogues

Quercetin analogues Q1 and Q2 were synthesized from 2–hydroxyacetophenone and 4–substituted benzaldehydes in two steps. The first step involves Claisen Schimdt reaction which resulted in the formation of the chalcone, followed by Algar–Finland–Oyamanda reaction resulting in the synthesis of the above flavonols.

A suspension of 4–chlorobenzaldehyde (1.36 g) (for Q1) /4–methoxybenzaldehyde (for Q2) and 2–hydroxyacetophenone (1.405 g) in ethanol (25 ml) was cooled to 10^{0}C and 7.5 ml of 40% w/v KOH solution was added drop wise. The reaction mixture was stirred for 18h at room temperature. Dichloromethane (125 ml) was added and

the organic layer was washed with H_2O (3x50 ml), dried over sodium sulphate and concentrated in vacuo. The oily residue was dissolved in ethanol (100 ml) and 5.4% (w/v) NaOH solution (30 ml) followed by drop wise addition of 4 ml of 35% H_2O_2. The reaction mixture was stirred in an ice bath for 3h and subsequently at room temperature for 12h resulting in a yellow suspension. After acidification with 2M HCl (30 ml), the precipitate was filtered and dried. The crude product was purified by passing it through silica gel column using chloroform as eluent, to give pure Q1 (4′–chloro–3–hydroxyflavone) and Q2 (4′–methoxy–3–hydroxyflavone).

Table 1: ^{1}H and ^{13}C NMR chemical shifts (ppm) for quercetin and its analogues in DMSO-d_6 at 323K

Assignment		Quercetin		Q1 ^{1}H	^{13}C	Q2	^{13}C
^{1}H	^{13}C	^{1}H	^{13}C			^{1}H	
	C2		147.4		144.5		146.1
H5	C3	6.22(s)	136.2	7.74(d)	134.9	7.74(d)	133.9
H6	C4	6.44(s)	176.4	7.49(t)	173.4	7.47(t)	173.2
H7	C5	7.70(s)	161.2	7.81(t)	134.1	7.79(t)	138.5
H8	C6	6.91(d)	98.7	8.12(d)	129.7	8.12(d)	114.5
H2′	C7	7.58(d)	164.4	8.26(s)	129.7	8.21(s)	114.5
H3′	C8	9.18(s)	93.8	7.64(s)	118.8	7.15(s)	118.6
H5′	C9	12.46(s)	157.0	7.62(s)	155.0	7.13(s)	154.9
H6′	C10	10.70(s)	98.7	8.24(s)	121.7	8.19(s)	121.8
3–OH	C1′	9.18(s)	122.5	9.63(s)	139.6	9.26(s)	124.9
5–OH	C2′	9.18(s)	115.6		125.2	3.87(s)	125.1
7–OH	C3′		145.5		130.6		125.1
3′–OH	C5′		116.1		130.6		129.8
4′–OH	C6′		115.7		125.0		160.9
4′–OCH_3	C4′		148.2		129.0		56.0
	CH_3						

The analogues thus prepared were characterized by their elemental analysis and ^{1}H, ^{13}C and 2D COSY NMR spectral data. The ^{1}H and ^{13}C NMR chemical shifts of the quercetin, Q1 and Q2 in DMSO–d_6 at 323 K are given in Table 1.

RESULTS AND DISCUSSION

Molecular dynamic simulations

During the entire simulation, there are no significant drifts in the temperature, pressure or the box size indicating that the lipid bilayer are well equilibrated. The movement of the molecule and formation of hydrogen bonds are monitored during the complete 20 ns simulation time (Fig. 2).

It is observed that in each case, molecules move from the centre of the bilayer towards the polar head group region and form hydrogen bonds. However, the trajectory analysis shows large differences in three cases (Fig. 3).

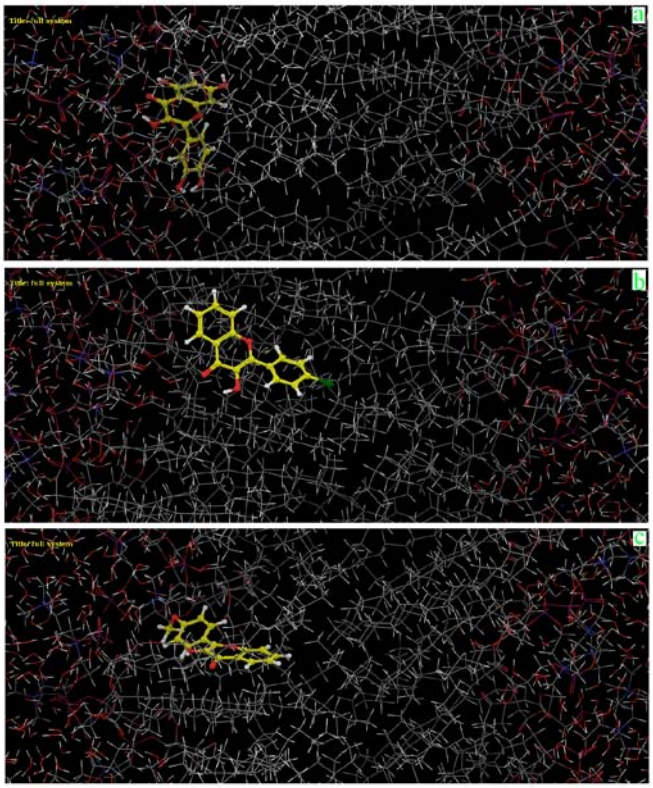

Fig. 2: A snapshot of 20 ns MD simulations of drug/analogue –DPPC system (a) quercetin, (b) Q1and (c) Q2. In each figure, the molecules incorporated are shown in yellow color with oxygen atoms in red. Nitrogen atoms of polar head region of lipid are shown in blue, oxygens in red and alkyl chains in white.

Quercetin starts moving towards the polar head region and forms the first hydrogen bond with the head region in less than 0.5 ns. Further movement of quercetin molecule along the 20 ns trajectory results in an increase in the number of such hydrogen bonds (Fig. 3a) giving rise to a maximum of four hydrogen bonds formed between quercetin and DPPC molecules. Out of this the 4´–OH group in the B ring involved in the hydrogen bond formation for maximum number of times (93%). This is followed by the 3´–OH group (73%) and 7–OH group (56%). On a few occasions, involvement of either 3–OH or 5–OH is also observed. In contrast, Q2 although moves towards polar head region.

The maximum number of hydrogen bonds formed is only two, involving 3–OH and 4´–OCH_3 groups (Fig. 3c). In the case of Q1, H–bond formation is observed only on a few occasions between the 3–OH group and the head region of lipid (Fig. 3b).

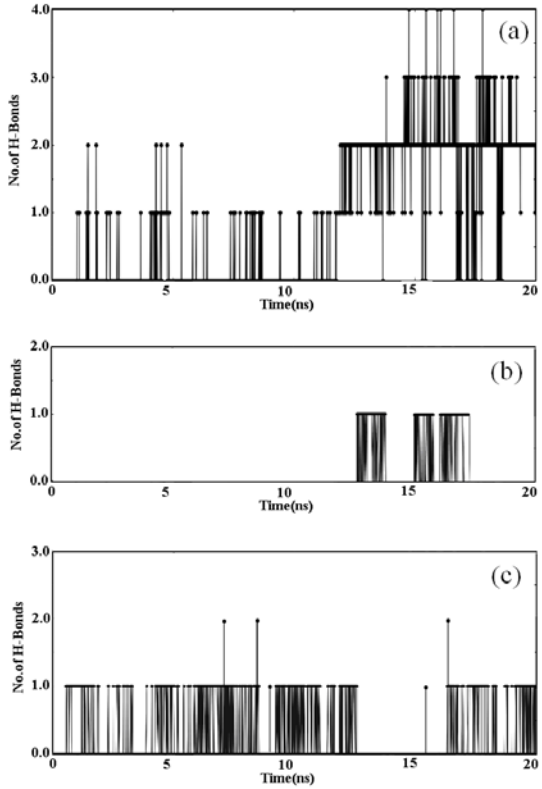

Fig. 3: Hydrogen bond formation as a function of time. X –axis shows the time (ns) during which the entire simulations were carried out. Y–axis shows number of H–bonds observed between (a) quercetin, (b) Q1, (c) Q2 and DPPC at a given point of time.

Due to high hydrocarbon content and large size of the molecule, coupled with hydrogen bond formation with the polar head of DPPC, quercetin gets located and stabilizes at the lipid/water interfacial region during the entire simulation. The interface location is the most probable location for quercetin as shown in Fig. 2a. Q2 is also observed to be located in the interfacial region. However, due to less number and less frequent hydrogen bonds it does not remain at the interface but penetrates in the hydrophobic core of the bilayer (Fig. 2c). Q1 on the other hand is located mostly into the hydrophobic region.

The solubility of quercetin is the rate limiting factor in absorption. Attempts to improve water solubility are major approaches in the structural modifications of quercetin. However, the water soluble derivatives of quercetin also do not show bioavailability of more than 20% indicating that there are other factors responsible [29]. One of the major factors associated with absorption is crossing over the lipid bilayers which involve passage of the drug across the hydrophilic as well as the hydrophobic region. Formation of hydrogen bonds at the polar head region provides an energy barrier which has to be overcome in order to enter the hydrophobic core.

During the entire 20 ns of simulation time, it is observed that quercetin remains associated with the polar head group region and is not able to overcome the hydrogen bonding barrier to enter the hydrophobic core of the lipid bilayer suggesting a rate limiting factor in the absorption of quercetin. For Q1 and Q2, the number of hydrogen bonds formed is comparatively less (1 and 2 in case of Q1 and Q2, respectively as against 4 for quercetin;, these molecules may present lower energy barriers to enter hydrophobic core of the bilayer and therefore permeation across the membrane is likely to be easier.

In this context, it is important to cite the example of the drug verapamil which during MD simulation, forms 4 hydrogen bonds similar to quercetin, and is therefore unable to enter the hydrobhobic core of the lipid bilayer [30]. A transporter such as P–glycoprotein is used to facilitate its permeation across the membrane. There are reports indicating a possible active transport of quercetin involving different transporters [31]. Our results from MD simulation also indicate possible existence of an active transport mechanism involving a transporter protein enabling quercetin to cross the lipid bilayer.

Binding studies with MLVs

Fig. 4 shows the plot of fraction of drug/analogues bound to MLVs with increasing concentration of lipid. It is observed that there is an increase in binding affinity of quercetin, Q1 and Q2 with increasing concentration of lipid. In case of quercetin, nearly 56%, and in Q2 67% binding is observed even at relatively low (0.25mM) concentration of lipid. On the other hand, total drug bound in case of Q1 is only 47% at the same lipid concentration. After a certain concentration of lipid the binding curves show a plateau.

The apparent binding constants measured are, quercetin–10710M^{-1}, Q1– 9620M^{-1} and Q2– 12000M^{-1}. A plot of the inverse of the fraction of drug bound versus the inverse of the lipid concentration (inset in Fig. 4) is linear. The results indicate that these molecules bind to the MLVs with variable degree of affinity in the order Q2 > quercetin >

Q1. The extent of binding may be due to differences in the number of hydroxyl groups and types of substituents present in the three cases. It further supports the results where Q1 does not show any binding to the polar head region as compared to quercetin which is strongly bound to head region. Q2 might have binding involving both hydrophobic as well as polar region of the lipid bilayer.

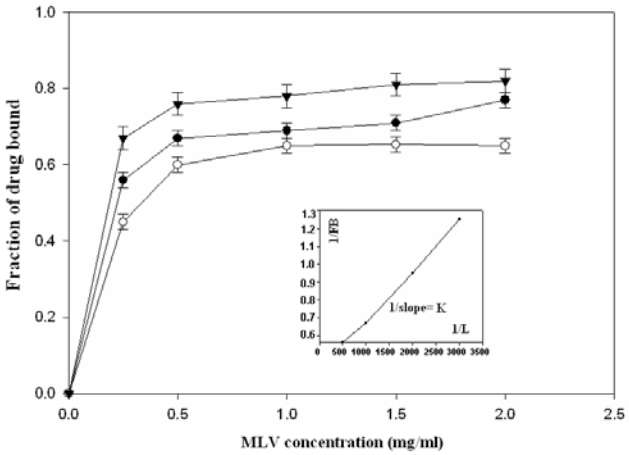

Fig. 4: Binding of quercetin (●), Q1 (○ and Q2 (▼) with DPPCMLVs (pH 7.2). The fraction bound is determined by the centrifugation method, as described in section 2. Inset shows the double reciprocal plot.

DSC studies

Differential scanning calorimetry is a sensitive technique for studying the effect of the drug on the packing order of the lipid bilayers. The thermotropic aspect of drug–lipid interactions can be studied by examining the changes in the melting point and the shape of the DSC trace [32]. During heating, the lipid initially undergoes a pre–transition ($L_{\beta'}$–$P_{\beta'}$) from an ordered 'gel' state where the lipids are ordered and tilted ($L_{\beta'}$) to the $P_{\beta'}$ state where the lipids are still ordered and in a gel state but with a minimal tilt. The pre–transition occurs before the main transition and is smaller. During the main transition ($P_{\beta'}$–$L_{\alpha'}$) lipids undergo a change from the ordered state ($P_{\beta'}$) to a fluid disordered state L_{α}.

The multilamellar structure of plain DPPC shows a pre transition at 34.5ºC, which is an indication of the mobility of the polar head group of DPPC. The mobility of the alkyl chain is seen in the main transition (T_m) at 41.8ºC. It is known that the interaction between flavonoids and lipid bilayers leads to the fluidifying effect due to the introduction of lipophilic flavonoid molecules into the ordered structure of the lipid bilayers [33]. In fact, these molecules act as a spacer in lipid bilayer leading to a decrease in the T_m.

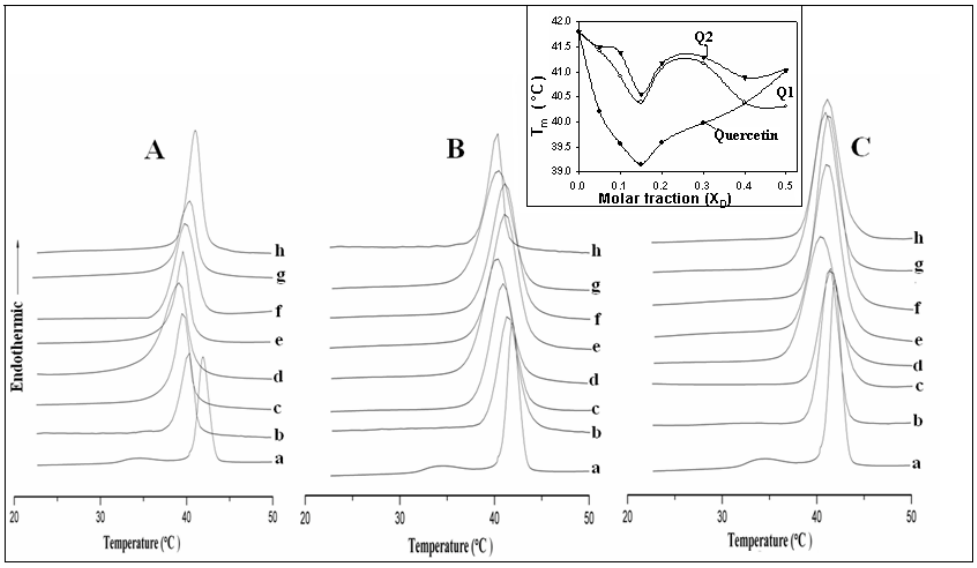

Fig. 5: DSC heating curves of hydrated DPPC MLVs (50mM) containing (A) quercetin (B) Q1 and (C) Q2, at the molar fractions: a=0.00; b=0.05; c=0.10; d=0.15; e=0.20; f=0.30; g=0.40; h=0.50. Inset figure shows the plot of T_m Vs molar fractions.

Effect of quercetin, Q1 and Q2 on DPPC bilayers

Figure 5 shows DSC thermogram of lipid bilayers incorporated with quercetin, Q1 and Q2. The lower graph (a) in each case represents the thermogram for lipid bilayers alone where the pre and the main transitions are observed at 34.5 C and 41.8 C, respectively. Curves b–h represent the lipid bilayer thermogram incorporated with increasing concentration of the three molecules.

In all the cases it is observed that the pre transition peak broadens beyond detection. Main transition on the other hand decreases to a lower value with increasing molar fraction until X_D=0.15 (inset in

Fig. 5). The decrease in main transition is maximum in case of quercetin (39.1ºC), followed by Q1 and Q2 (Table 2). At higher drug concentration, (X_D > 0.15), in all the three cases, the T_m starts moving towards higher temperature. This increase in T_m continues in case of quercetin with increasing molar fraction of the drug (X_D=0.25–0.50). In contrast, the increase in T_m in case of Q1 and Q2 is marginal and it further decreases after a short increase (inset Figure 5).

Table 2: Pre and main transition peaks (T_p and T_m) in ºC of DPPC dispersions at different molar fractions of quercetin, Q1 and Q2.

Molar fraction	Quercetin		Q1		Q2	
	T_p	T_m	T_p	T_m	T_p	T_m
0.00	34.54	41.80	34.54	41.80	34.54	41.80
0.05	35.26	40.21		41.42		41.50
0.10		39.56		40.91		41.38
0.15		39.15		40.39		40.56
0.20		39.56		41.08		41.17
0.30		39.97		41.17		41.30
0.40		40.37		40.39		40.89
0.50		41.02		40.31		41.05

The increase in T_m at higher drug concentration in case of quercetin is in agreement with an earlier report [34] where it has been suggested that below T_m, the quercetin molecules are less soluble in the rigid structure of the gel phase. As a result, further increase in concentration of the drug leads to aggregation [34]. The result of such a process is the exclusion of drug molecules from the homogeneous lipid–drug dispersion, causing an increase in T_m towards the values shown for the less perturbed lipid bilayer by lower molar fraction of the drug. Alternatively, the increase in T_m may be due to the tendency of the drug molecules to leave the lipid bilayer to the aqueous phase with time. However, no change in the T_m was observed even when the sample was scanned after 24h under identical conditions. From these results it is observed that although quercetin affects the pre– and main transitions, it excludes out (aggregates) at higher concentrations and beyond a certain concentration no further binding is expected. In contrast, Q1 and Q2 continue to enter the bilayer at higher concentration, and affect the bilayer transition.

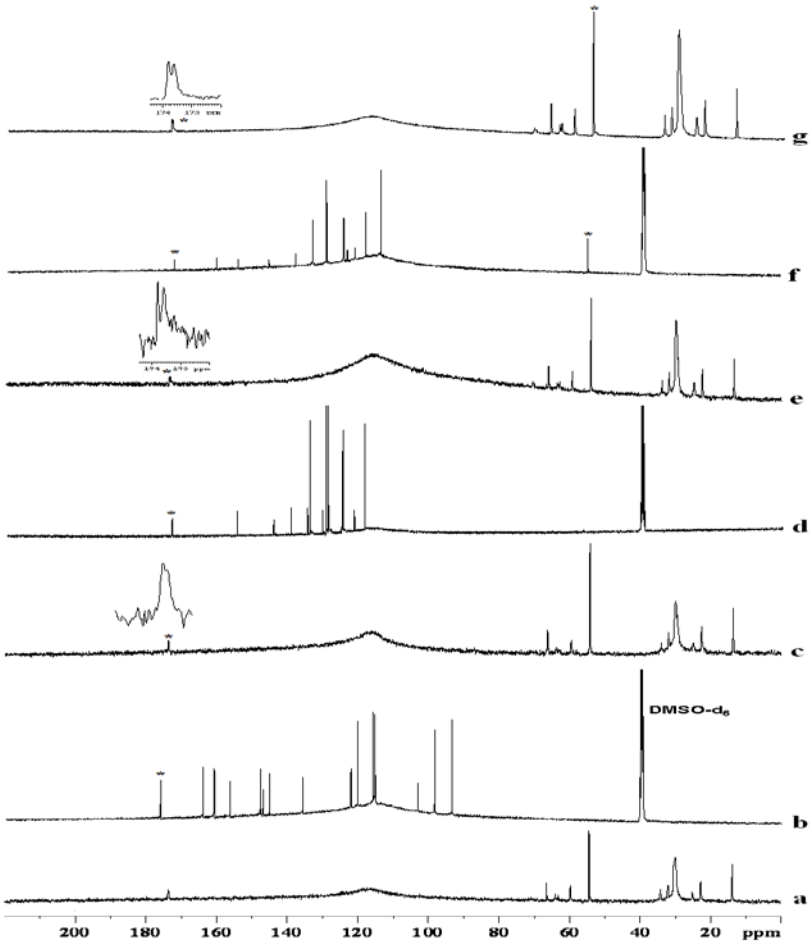

Fig. 6: 125.7 MHz ^{13}C NMR spectra of (a) DPPC ULVs in D_2O (b) quercetin (d) Q_1 (f) Q_2 in DMSO−d_6. Spectra (c), (e) and (g) show quercetin, Q1 and Q2 incorporated into DPPC ULVs (1:5 drug:lipid molar ratio) respectively at 323k. The drug peaks which remained sharp after incorporation into DPPC ULVs are indicated with *.

NMR experiments

^{13}C NMR

To probe deeper into the nature of the interaction between quercetin, ^{13}C NMR has been carried out for quercetin and its analogues alone (Fig. 6 (b, d and f)) and in the presence of the lipid bilayers (Fig. 6 (c, e and g)) in 1:5 drug:lipid molar ratio at 323 K. The three spectra from the drug/analogue are nearly identical except for the signals that appear due to the substituted methoxy group in case of Q2. The assignments have been made from the multiplicity pattern of the resonances (Table 1). The ^{13}C NMR spectrum of the DPPC bilayer (Fig. 6 a) has been assigned as reported in the literature [35].

It is observed that in the ^{13}C spectra of the DPPC ULV's incorporated with drug/analogues all the signals arising from quercetin, Q1 and Q2 are broadened (as compared to their pure form) with the exception of signal arising from >CO group in the ring C in all the three cases which remains sharp (Fig. 6). In case of Q2, another signal arising from –OCH3 group of ring B remains sharp and shifts upfield. The broadening of the signals arises due to an exchange at an intermediate time scale between the bound and free form. Due to the broadening of the signals, it is difficult to measure the spin lattice relaxation (T_1) and the spin–spin relaxation times (T_2), which are measures of the overall tumbling and segmental motions in the molecule. In the fast tumbling range, both T_1 and T_2 are large, typically of the order of 10 seconds [36]. The estimates of spin–spin relaxation times (T_2) from the NMR line–width indicate that the T_2 values are of the order of 100ms. Lower values of T_2 indicate that the molecules loose their mobility and become strongly bound to lipid bilayers resulting in a loss of motional freedom. This also indicates an increase in the motional ordering of the lipid acyl chain and head group. However, a few signals which remain relatively sharp indicate the mobility of the respective atoms.

It may be noted that the C=O peak of quercetin at 176.4 ppm shifts upfield by Δδ~2 ppm and appears as a shoulder peak to the C=O of the acyl group of the lipid at 173.83 ppm which also shows a small upfield shift of Δδ=0.03 ppm. This may be due to involvement of the C=O group or its neighbouring phenolic–OH group in hydrogen bond formation with the acyl group of polar head of lipid bilayer. However, in case of Q1 and Q2 the signal arising from C=O group does not show any change in chemical shift. In the spectrum of ULVs of DPPC incorporated with Q2 the signal arising from the methoxy carbon appears at 54.83 ppm which is upfield shifted by 1.17 ppm. This large change indicates its possible involvement in binding with the lipid bilayer.

The above results suggest that the quercetin forms hydrogen bond with the polar head group involving C=O group or its adjacent phenolic–OH group. In case of Q2, possibly methoxy group is involved in interaction. However in case of Q1 no such interaction is observed.

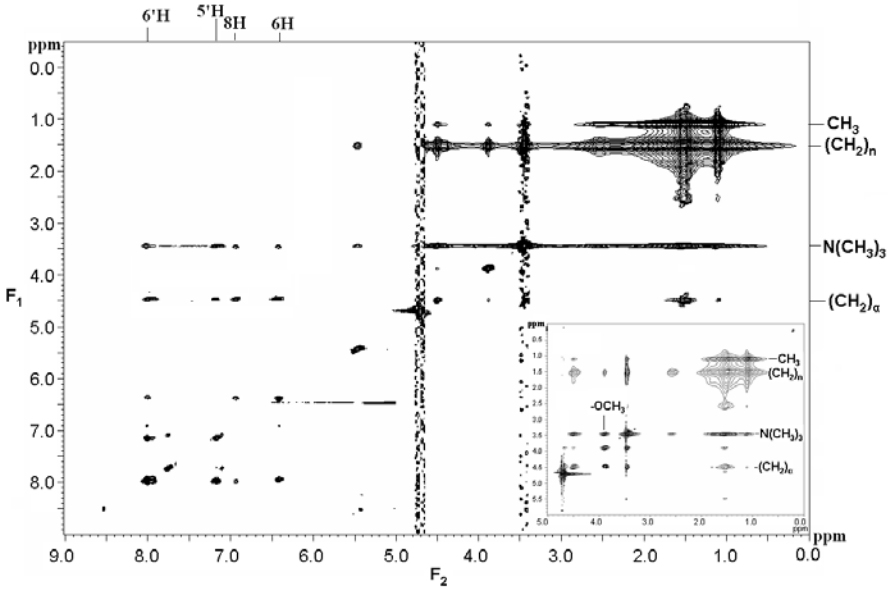

Fig. 7: 2D NOESY spectrum of DPPC ULVs at 323k incorporated with quercetin (1:5 molar ratio). Inset shows the portion of spectrum of DPPC ULVs incorporated with Q_2 (1:5 molar ratio) indicating NOEs arising from methoxy group of Q2.

2D NOESY

2D NOESY can be used for the analysis of the intermolecular interactions as well as the conformation of the molecules in the lipid bilayer. NOEs arise when the two atoms (within the molecule or from two different molecules) are at a distance≤ 5°A apart. The NOESY spectrum of quercetin incorporated into DPPC unilamellar vesicles is shown in Fig. 7. The assignments of NOEs between quercetin and lipid molecules are indicated along F2 and F1 dimensions, respectively. It is observed that protons at 5′, 6′, 6 and 8 positions of ring A and B of quercetin show NOEs with the head group protons (i.e $-N(CH_3)_3$ and $-(CH_2)\alpha$) of DPPC bilayer. This possibly arises due to the involvement of phenolic–OH groups of ring B and A in hydrogen bonds with the polar head group of lipid. In the case of Q2 incorporated with DPPC vesicles these interactions are completely absent as such phenolic–OH groups are absent and one of them is substituted by methoxy group. However, methoxy group shows NOEs with polar head group protons of lipid as indicated in inset of Figure 7. In the case of Q1 where there are no phenolic–OH groups present in the ring and there is chloro group in place of methoxy of Q2, there are no NOEs observed between the ring protons and the lipid head group.

These experimental results further support the MD simulation results wherein the hydroxyl groups of quercetin and the methoxy group of Q2 are involved in hydrogen bonding with the polar head group of the lipid bilayers.

^{31}P NMR

^{31}P NMR is a useful technique for the study of the polymorphic phase behavior of hydrated phospholipids in excess water as lipid phosphorus exihibit large chemical shift anisotropy. ^{31}P NMR line shape is sensitive to different types of motion of lipid molecules. The dynamics of phopholipid bilayer system consists primarily of rapid rotation of the lipid molecules about their long axes. The ^{31}P NMR resonance line shape is determined by the chemical shift

anisotropy (CSA) of the phosphate group coupled with the molecular motions near the head groups [37, 38]. Lipid bilayers have a characteristic broad spectrum with a high field peak and low field shoulder [39, 40]. The CSA can be measured from the low and high field (the $\sigma_{\parallel}$ and $\sigma_{\perp}$ components) shoulders of the spectrum.

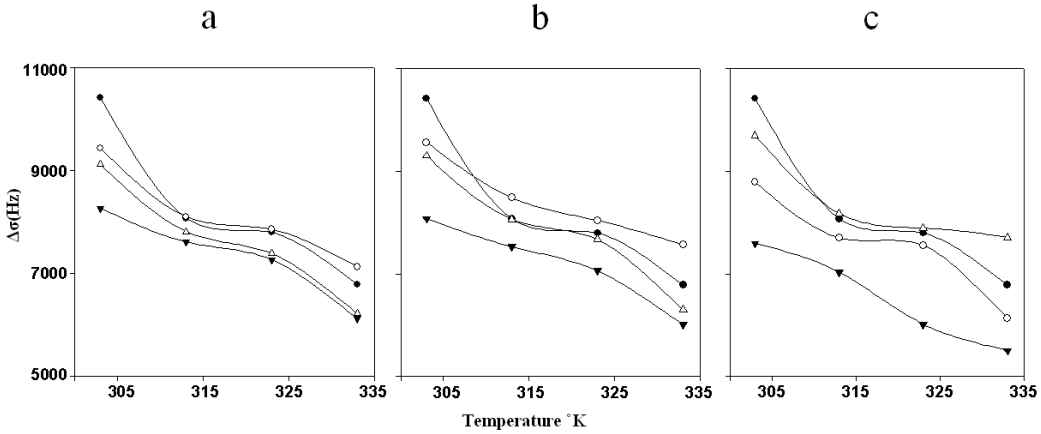

Fig. 8: Change in CSA (Hz) represented by $\Delta\sigma=\sigma_{\perp}-\sigma_{\perp}$ with temperature at (a) 1:10 (b) 1:5 and (c) 1:2 drug:lipid molar ratios. DPPC MLVs (●), quercetin (○ Q1 (◂) and Q2 (△).

The effect of quercetin, Q1 and Q2 on the ^{31}P NMR line shape was measured as a function of concentration as well as temperature. ^{31}P NMR spectra of DPPC MLVs incorporated with quercetin, Q1 and Q2 at different drug:lipid molar ratios have been recorded at temperatures 303K to 333K (Figure not shown). The change in CSA with temperature is shown in Figure 8. Higher temperature is known to enhance the fluidity of the MLVs resulting an overall decrease in CSA in all the cases. All the three molecules further change the CSA value as compared to pure DPPC MLVs at all the three drug:lipid molar ratios (Fig. 8). In case of quercetin, with increasing concentration of drug, the change in CSA with temperature increases marginally up to 1:5 drug:lipid ratio (Fig. 8a and 8b) as compared to DPPC MLVs and further CSA decreases at 1:2 drug:lipid ratio (Fig. 8c). This is in agreement with the DSC results where at higher concentration the drug tends to aggregate giving rise to an increase in transition temperature. The marginal change in CSA further indicates that the binding of the molecule to the lipid as observed from MD and DSC studies, though may be rigid, the effect on CSA gets compensated due to the increase in fluidity of MLVs in presence of drug. These results are further substantiated by the reports on rigidifying effect of quercetin and anti-cancer dietary factors on liposomal membranes [41, 42]

The effect of Q1 and Q2 on CSA with higher temperature at the three concentrations is indicated in Figure 8 (a, b and c). It is observed that at all the concentrations; the increase in CSA is more in case of Q2 as compared to Q1. This is possibly due to the binding of Q2 with the head group which imparts more rigidity as compared to Q1. It may be noted that the bilayer features of DPPC MLVs do not change in presence of quercetin, Q1 and Q2 (Figure not shown) and there is no polymorphism observed.

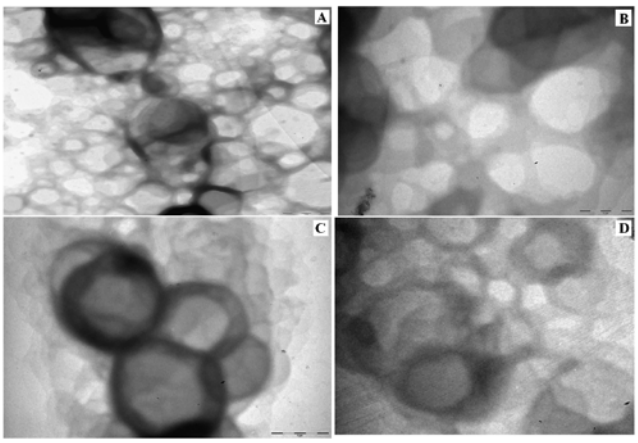

Fig. 9: TEM pictures of DPPC MLVs (A), and incorporated with quercetin (B) Q1 (C) and Q2 (D)) in 1:5 drug:lipid molar ratio.

TEM

TEM is an important tool to gain information on liposomes, as well as on the morphological changes taking place upon interaction with drugs, surfactants, DNA and other polyelectrolytes [43]. We have studied the phase behavior and the aggregate structure of liposomes using TEM. Figure 9 shows electron micrograph of DPPC dispersions alone and in presence of drugs at 1: 5 drug:lipid molar ratio. It is observed that pure DPPC dispersions show the characteristic bilayer features (Fig. 9A) [44]. In presence of quercetin, large aggregates of lipid dispersions are observed (Fig. 9B). These types of large aggregates appear relatively well separated with an even corrugated surface as reported earlier [45].

The TEM pictures of lipid vesicles incorporated with Q1 and Q2 do not show a large change in the size of lipid vesicles (Fig. 9 C and D). These results indicate that the drugs bind to the cell membrane such that they stabilize the bilayer character of the membrane and thus prevent the cell–cell fusion [46] which is an important phenomenon for drug entry in the membrane.

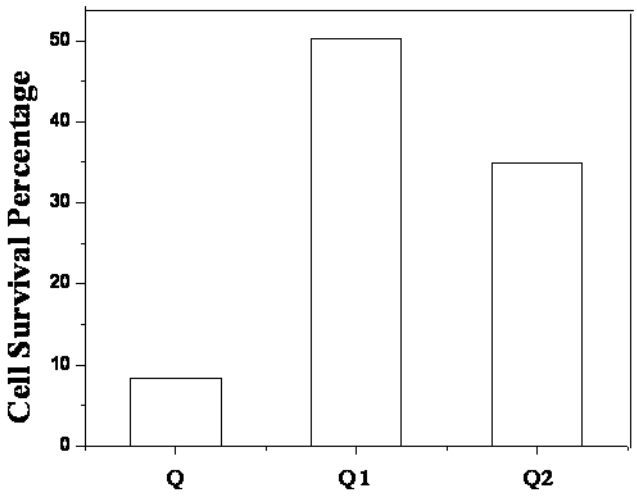

Fig. 10: Cell survival percent in breast cancer cell line (MCF-7) in presence of Q, Q1 and Q2 using SRB assay as described in Section 2.8.

Anticancer activity

The anticancer activities of Q1 and Q2 have been compared with that of quercetin against the breast cancer cell line (MCF-7). It is observed that quercetin is effective to a large extent with 12.8% cell survival. Quercetin analogs, Q1 and Q2 also show significant activity with 50.3% and 25.0% cell survival, respectively (Fig. 10). The results thus indicate that the phenolic hydroxyl groups are not the only factor responsible for the antiproliferative activity.

CONCLUSIONS

The modified analogues Q1 and Q2 of quercetin interact with head group of DPPC model membrane to different extent and thereby may have different membrane permeability. Quercetin interacts with the hydrophillic head group of DPPC model membrane involving phenolic–OH groups present at positions 3′, 4′ of ring B and position 7 of ring A. This brings the neighboring atoms in close proximity to the head group of lipid as observed from NOE experiments. This is supported by MD simulations whereby maximum number of hydrogen bonds is formed between the polar head group of lipid and the phenolic hydroxyl groups of quercetin. It is proposed that removal of –OH groups may decrease the energy barrier and enhance the entry/permeability of quercetin in the membranes. Accordingly, the interaction of analogue Q2 involves only the methoxy group in the binding and more susceptible to permeation. In case of Q1, the interaction with the head group (at the lipid water interface) is minimal. The results are supported by MD simulation studies.

The findings are corroborated by the binding of these molecules with DPPC membrane and their effect on fluidity using DSC. Higher concentration of quercetin is not acceptable to the membrane structure as observed from DSC results. This is correlated with the fact that excess amount of quercetin exerts oxidative effect [47].

Our results indicate that the different substituents in the quercetin ring may have different effect on membrane permeability. As the interaction of the molecule with polar head group decreases, the energy barrier reduces and permeation may become more facile. In the present case, quercetin poses high energy barrier due to strong binding with the polar head group of lipid. Q1 does not bind to the head group at all and remains in the hydrophobic core so may not result in crossing the hydrophilic lipid-water interface. On the other hand, Q2 involves both hydrophilic as well as hydrophobic interaction thereby well suited for membrane permeation.

Results of anticancer activity further indicate that modification of quercetin retains the antiproliferative activity to a large extent while increasing the permeability and thereby bioavailabilty. Therefore, analogue Q2 may be proposed to be a promising candidate and can act as a base for further structural modifications of quercetin in search of better bioavailability.

ACKNOWLDGEMENT

NMR work carried out at the National Facility for High Field NMR located at TIFR is gratefully acknowledged. R. Sinha and G. Govil thank the Indian National Science Academy and Urmila J. Joshi thanks All India Council for Technical Education for funding. The help provided by K. Ray, S. Shirolikar and L. Borde at the Cryo TEM facility and A. Juvekar at ACTREC, Mumbai, for anticancer activity test is also acknowledged.

REFERENCES

1. Rice-Evans CA, Miller NJ, Paganga G, Structure-antioxidant activity relationships of flavonoids and phenolic acids, Free Radic. Biol. Med. 1996;20 : 933–956.
2. Van Acker SA, van Den Berg DJ, Tromp MN, Griffioen DH, van Bennekom WP, van der Vijgh WJ, Bast A, Structural aspects of antioxidant activity of flavonoids, Free Radic. Biol. Med. 1996: 20: 331–342.
3. Lautraite S, Musonda AC, Doehmer J, Edwards GO, Chipman JK, Flavonoids inhibit genetic toxicity produced by carcinogens in cells expressing CYP1A2 and CYP1A1, Mutagenesis 2002; 17:45–53.
4. Mutoh M, Takashi M, Fukuda K, Komatsu H, Enya T, Masushima-Hibiya Y, Mutoh H, Sugimura T, Wakabayashi K, Suppression by flavonoids of cyclooxygenase-2 promoter-dependent transcriptional activity in colon cancer cells: structure-activity relationship, Jpn. J. Cancer Res. 2000; 91: 686–691.
5. So FV, Guthrie N, Chambers AF, Moussa M, Carroll KK, Inhibition of human breast cancer cell proliferation and delay of mammary tumorigenesis by flavonoids and citrus juices, Nutr. Cancer 1996;26 :167–181.
6. Kang ZC, Tsai SJ, Lee H, Quercetin inhibits benzopyrene-induced DNA adducts in human Hep G2 cells by altering cytochrome P-450 1A1 gene expression, Nutr. Cancer 1999;35175–179.
7. Petelska BS, Figaszewski Z, Lewandowski W, Mechanisms of transport across cell membranes of complexes contained in antitumour drugs, Intl. J. Pharm. 2001;222: 169–182.
8. Yang CY, Cai S J, Liu H, Pidgeon C, Immobilized artificial membranes–screen for drug membrane interactions, Adv. Drug Del. Rev. 1997; 23:29–256.
9. Hausen H , Poupartm G, In: P. Yeagle, The Structure of Biological Membranes, CRC Press, London, 3 (1992).
10. Mastrobattista E, Koning GA, Storm G, Immunoliposomes for targeting anti-cancer drugs, Adv. Drug Del. Rev. 1999; 40:103–127.

11. Frezard F, Liposomes: from biophysics to the design of peptide vaccines, Braz. J. Med. Biol. Res. 1999; 32:181–189.
12. Huang CH, Li S, Calorimetric and molecular mechanics studies of the thermotropic phase behavior of membrane phospholipids, Biochem. Biophys. Acta 1999;1422: 273–307.
13. Fiasson KG, Fiasson JL, Waton H, Quercetin glycosides from European Ranunculus species of subgenus Batrachium , Phytochem. 1997;45:1063–1067.
14. Karakaya S, Bioavailability of Phenolic Compounds, Critical Reviews in Food Science and Nutrition, 2004; 44:453–464.
15. Cabrera M, Simoens M, Falchi G, Lavaggi ML, Piro OE, Castellano EE, Vidal A, Azqueta A, Monge A, Lo´pez de Cera A, Sagrera G, Seoane G, Cerecetto H, Gonza´lez M, Synthetic chalcones, flavanones, and flavones as antitumoral agents: Biological evaluation and structure–activity relationships, Bioorganic & Medicinal Chemistry 2007; 15: 3356–3367.
16. Hu K, Wang W, Cheng H, Pan S, Ren J, Synthesis and cytotoxicity of novel chrysin derivatives, Med Chem Res 2011; 20: 838–846.
17. Ollila F, Halling K, Vuorela P, Vuorela H, Slotte P, Characterization of Flavonoid-Biomembrane Interactions, Arch. Biochem. Biophys. 2002;399: 103–108.
18. Aue WP, Bartholdi E, Ernst RR, Two-dimensional spectroscopy-application to nuclear magnetic resonance, J. Chem. Phys. 1976;64: 2229–2246.
19. Bazzo R, Edge CJ, Wormald MR, Rademacher TW, Dwek RA , Full simulation of ROESY, including the Hartman Hahn effects, Chem. Phys. Lett. 1990;174: 313–319.
20. Kornberg RD, McConnell HM, Inside-outside transitions of phospholipids in vesicle membranes, Biochemistry 1971;10: 1111–1120.
21. Cheng HY, Randall CS, Holl WW, Constantinides PP, Yue TL, Feuerstein GZ, Carvedilol-liposome interaction: evidence for strong association with the hydrophobic region of the lipid bilayers, Biochem. Biophys. Acta 1996;1284: 20–28.
22. Nagle JF, Zhang R, Tristam-Nagle S, Sun W, Petrache HI, Suter RM, X–ray structure determination of fully hydrated *Lα*–phase dipalmitoyl phosphati –dylcholine bilayers, Biophys. J. 1996;70: 1419–1431.
23. dos Santos DJV A, Saenz-Me´ndez P, Eriksson LA, Guedes RC, Properties and behaviour of tetracyclic allopsoralen derivatives inside a DPPC lipid bilayer model, Phys. Chem. Chem. Phys. 2011;13: 10174–10182.
24. dos Santos DJVA, Eriksson LA, Permeablity of psoralen derivatives in lipid membranes, Biophysical J. 2006;91: 2464.
25. Erdtman E, dos Santos DJVA, Löfgren L, Eriksson L A, Modelling the behavior of 5-aminolevulinic acid and its alkyl esters in a lipid bilayer' Chem. Phys. Lett. 2008;463: 178.
26. Eriksson ESE, . dos Santos DJVA, Guedes RC, Eriksson LA, Properties and permeability of hypericin and brominated hypericin in lipid membranes, J. Chem. Theory Comput., 2009;5: 3139–3149.
27. Skehn P, Storeng R, Scudiero A, Monks J, McMohan D, Vistica D, Jonathan TW, Bokesch H, Kenney S, Boyd MR, New colorimetric cytotoxicity assay for anticancer drug screening, J. Natl. Cancer Inst. 1990;82: 1107–1112.
28. Nagle JF, Zhang R, Tristam-Nagle S, Sun W, Petrache HI, Suter RM, X–ray structure determination of fully hydrated *Lα*–phase dipalmitoyl phosphatidylcholine bilayers, Biophys. J. 1996;70: 1419–1431.
29. Hu M, Commentary: Bioavailability of Flavonoids and Polyphenols: Call to Arms, Mol. Pharm. 2007;4: 803–806.
30. Walgren RA, Lin J, Kinne RKH and Walle T, Cellular uptake of dietry flavonoid quercetin 49-b-Glucoside by sodium-dependent glucose transporter SGLT1, J. Pharmacol.Exp. Ther. 2000;294: 837–843.
31. Cunningham P, Ahmed IA, Naftalin RJ, Docking studies show that D-glucose and quercetin slide through the transporter GLUT1, J. Biol. Chem. 2005;281: 5797–5803.
32. Lambros MP, Sheu E, Lin JS, Pereira HA, Interaction of a synthetic peptide based on the neutrophil derived antimicrobial protein CAP 37 with dipalmitoyl-phosphatidylcholine membranes, Biochem. Biophys. Acta 1997;1329: 285–290
33. Jain MK, Order and dynamics in bilayers, solute in bilayers. In Jain MK Ed;, Introduction to Biological Membranes, Wiley, New York, 1988, PP.122–165.
34. Saija A, Bonina F, Trombetta D, Tomaino A, Montenegro L, Smeriglio P and Castelli F, Flavone-Biomembrane Interactions: A calorimetric study on dipalmitoylphosphatidylcholine vesicles, Intl. J. Pharma. 1995; 124 :1–8.
35. Levine YK, Partington P, Roberts GCK, Birdstall NJM, Metcalfe JC, ^{13}C Nuclear magnetic relaxation times and models for chain motion in lecithin vesicles, FEBS Lett. 1972; 23: 203–207.
36. Neumann JM, Zachowski A, Tran-Dinh S, Devaux PF, High resolution proton magnetic resonance of sonicated phospholipids, Eur. Biophys. J. 1985; 11: 219–233.
37. Pawar B, Kanyankar MA, Pissulenkar R, Joshi M, Coutinho EC, Srivastava S, Probing molecular level interaction of antifungal drugs with model membranes by molecular modeling, multinuclear NMR and DSC methods, Intl. J. Curr. Pharm. Res. 2010; 2: 47–56.
38. D'Souza C, Kanyalkar M, Joshi M, Coutino E, Srivastava S, Search for novel neuraminidase inhibitors: Design, synthesis and interaction of oseltamivir derivatives with model membrane using docking, NMR and DSC methods, Biochem. Biophys. Acta 2009;1788:1740–1751.
39. Waghmare A, Kanyalkar M, Joshi M, Srivastava S, In-vitro metabolic inhibition and antifertility effect facilitated by membrane alteration: search for novel antifertility agent using nifedipine analogues, Eur. J. Med. Chem. doi: 10.1016/j.ejmech.2011.05.022J.
40. Frenzel K, Arnold P, Nuhn, Calorimetric, ^{13}C NMR and ^{31}P NMR studies on the interaction of some phenothiazine derivatives with dipalmitoyl phosphatidylcholine model membranes, Biochem. Biophys. Acta 1978; 507:185–197.
41. Tsuchiya H, Nagayama M, Tanaka T, Furusawa M, Kashimata M, Takeuchi H, Membrane-rigidifying effects of anti-cancer dietary factors, Biofactore, 2002;16:45–56.
42. Tarahovsky YS, Muzafarov EN., Kim YA, Rafts making and rafts braking: how plant flavonoids may control membrane heterogeneity, Molecular and Cellular Biochemistry 2008; 314 65-71.
43. Srivastava S, Phadke RS, Govil G, Role of tryptophan in inducing polymorphic phase formation in lipid dispersion, Ind. J. Biochem. Biophys. 1988; 25:283–286.
44. D'Souza C, Kanyalkar M, Joshi M, Coutino E, Srivastava S, Probing molecular level interaction of oseltamivir with H5N1-NA and model membranes by molecular docking, multinuclear NMR and DSC methods, Biochem. Biophys. Acta 2009; 1788 484–494.
45. M Johnsson, K Edwards, Liposomes, disks and spherical micelles: Aggregate structure in mixtures of gel phase phosphatidylcholines and poly ethylene glycol;-phospholipids, Biophys. J. 2003; 85:3839–3847.
46. Chakraborty H, Chakraborty P K, Raha S, Mandal PC, M. Sarkar, Interaction of piroxicam with mitochondrial membrane and cytochrome c, Biochem. Biophys. Acta 2007; 1768:1138–1146.
47. Kohn A., Permeability to inhibitors of protein synthesis in virus infected cells, Adv. Viral Res. 1979;24:223–276.